Index modulation multiple access-aided multi-user VLC for Internet of Medical Things

ZHIHONG ZENG, 1,† D YUHAN DU, 2,3,† YANGPING QIAN, 4,5 MIN LIU, 1 AND CHEN CHEN^{1,6} D

Abstract: The Internet of Medical Things (IoMT), an extension of the Internet of Things (IoT) focused on healthcare, plays a vital role in enabling continuous monitoring of various medical activities. To address the increasing need for smart medical device connectivity, visible light communication (VLC) has emerged as a promising solution. In this paper, we propose and experimentally demonstrate a multi-user VLC system using an index modulation multiple access (IMMA) scheme tailored for IoMT. By addressing the diverse quality of service (QoS) requirements of different users, the IMMA scheme transmits data for low-speed users via index symbols and for high-speed users via constellation symbols, while significantly reducing the receiver's computational complexity compared to successive interference cancellation (SIC) in non-orthogonal multiple access (NOMA). The effectiveness of the IMMA scheme has been validated through both simulations and hardware experiments, with bit error rate (BER) performance compared against orthogonal frequency division multiple access (OFDMA) and under varying user separations. Experimental results show that the IMMA scheme outperforms the benchmark schemes and achieves significant distance extensions in a two-user VLC system.

© 2024 Optica Publishing Group under the terms of the Optica Open Access Publishing Agreement

1. Introduction

The Internet of Things (IoT) plays a pivotal role in improving quality of life by facilitating the continuous monitoring of various activities. In healthcare, the efficient use of IoT ensures prompt and accurate medical interventions, which is crucial for enhancing patient outcomes. This has led to the rise of the Internet of Medical Things (IoMT), a specialized extension of IoT focused on healthcare [1]. IoMT is designed to guarantee the availability of proper medical services, both in routine healthcare and critical situations such as the COVID-19 pandemic [2]. With the rapid growth of IoMT, there is an increasing global demand for large-scale smart device connectivity and high-speed wireless communication. However, due to the growing congestion of spectrum resources, traditional radio frequency (RF) communication may soon struggle to handle the surging mobile data traffic. Recently, optical wireless communication (OWC) using visible light, infrared, or ultraviolet bands has emerged as a promising solution to mitigate RF spectrum congestion [3-5]. Among OWC technologies, visible light communication (VLC), which utilizes commercially available light-emitting diodes (LEDs), offers several advantages such as abundant, unregulated spectrum resources, no electromagnetic interference (EMI), and enhanced physical-layer security, drawing considerable attention. As a result, VLC is widely seen as an effective complement to traditional RF communication for establishing high-speed, high-capacity networks [6]. Owing to its capabilities to support EMI-free wireless data transmission with broad

#544415 Journal © 2024

 $^{^{}I}$ School of Microelectronics and Communication Engineering, Chongqing University, Chongqing 400044,

²Chongqing Health Center for Women and Children, Chongqing 401147, China

³Women and Children's Hospital of Chongging Medical University, Chongging 401147, China

⁴China Merchants Testing Vehicle Technology Research Institute Co., Ltd., Chongqing 401329, China

⁵202112131028t@cqu.edu.cn

⁶c.chen@cqu.edu.cn

[†]These authors contributed equally to this work

bandwidth and large capacity, VLC has revealed its great potential for various IoMT applications such as mobile health–monitoring, medical data transmission and low-latency telemedicine [7–10].

In practical VLC-based IoMT (VLC-IoMT) systems, it is often required to connect multiple users within the coverage area of a single LED access point (AP). Therefore, the AP must be capable of transmitting information to several users simultaneously, making the design of an efficient multiple access technique crucial for multi-user VLC systems. Numerous multiple access methods have been proposed in the literature, with orthogonal frequency division multiple access (OFDMA) and non-orthogonal multiple access (NOMA) being the most commonly utilized [11–14]. In OFDMA-based systems, the available modulation bandwidth is divided and allocated to individual users, effectively preventing mutual interference. However, the spectrum partitioning results in a limited bandwidth for each user, significantly reducing the achievable data rate. In contrast, NOMA allows multiple users to simultaneously share the entire time and frequency resources by employing power domain superposition coding (SPC) and successive interference cancellation (SIC) [15]. While NOMA can improve spectrum utilization, the complexity of implementing SIC at the receiver side poses a challenge, especially for users with constrained communication and computational capabilities. Additionally, in real-world systems, different users often have varying quality-of-service (QoS) requirements. These users can typically be divided into two categories: one category includes users with limited computational capability and low data rate requirements such as environment sensors and health monitors, while the other category consists of high-speed users such as multimedia-capable mobile phones. Therefore, it is essential to consider these diverse QoS requirements when designing multiple access techniques for multi-user VLC-IoMT systems.

Recently, index modulation (IM) has attracted significant attention due to its advantages in spectrum and energy efficiency, as well as its hardware simplicity [16–18]. As a spectrum-efficient digital modulation technique, IM utilizes the indices of system building blocks to encode additional information bits, offering an alternative approach compared to traditional digital modulation methods. Given its excellent performance in spectral efficiency, IM has already been applied into orthogonal frequency division multiplexing (OFDM)-based communication systems [19]. Studies have shown that OFDM with index modulation (OFDM-IM) provides better bit error rate (BER) performance than conventional OFDM [20–22]. In OFDM-IM, information is transmitted not only via constellation symbols but also through the indices of subcarriers. Specifically, a subset of available subcarriers is selectively activated to transmit *M*-ary constellation symbols, while the remaining subcarriers are set to zero and not utilized for conventional modulation. Additionally, it is important to note that the data rate for transmitting index symbols is relatively low and fixed, whereas the data rate for constellation symbols is generally higher. Therefore, spectral-efficient OFDM-IM holds great potential as a candidate for practical multi-user VLC-IoMT systems.

In this paper, we propose, for the first time, a novel index modulation multiple access (IMMA) scheme for practical multi-user VLC-IoMT systems. The IMMA scheme takes into account the communication and computational capabilities, as well as the quality-of-service (QoS) requirements, of different users. Specifically, the detectors at the receiver can be significantly simplified, reducing computational complexity. The feasibility and superiority of the proposed IMMA scheme over conventional NOMA and OFDMA schemes have been successfully demonstrated through both simulation and experimental results.

2. Principle of IMMA

In this section, we describe the principle of the proposed IMMA scheme for VLC-IoMT systems. For simplicity and without loss of generality, a two-user VLC-IoMT system is considered here. Figures 1(a) and 1(b) illustrate the schematic diagrams of the IMMA transmitter and receiver,

respectively. At the transmitter, the input bits for each user are first divided into G groups using a bit splitter. The partitioned bits for user 1 and user 2 are then fed into an index selector and a constellation mapper to generate an OFDM subblock, respectively. Thus, each group's OFDM subblock consists of index bits and constellation bits with a length of N, where $N = N_{\rm data}/G$, and $N_{\rm data}$ represents the number of data subcarriers. Next, the G subblocks are concatenated by an OFDM block creator to form a complete OFDM block. Furthermore, inverse fast Fourier transform (IFFT) with a Hermitian symmetry (HS) constraint is applied to generate a real-valued OFDM signal. Finally, the transmitted signal is obtained after parallel-to-serial (P/S) conversion.

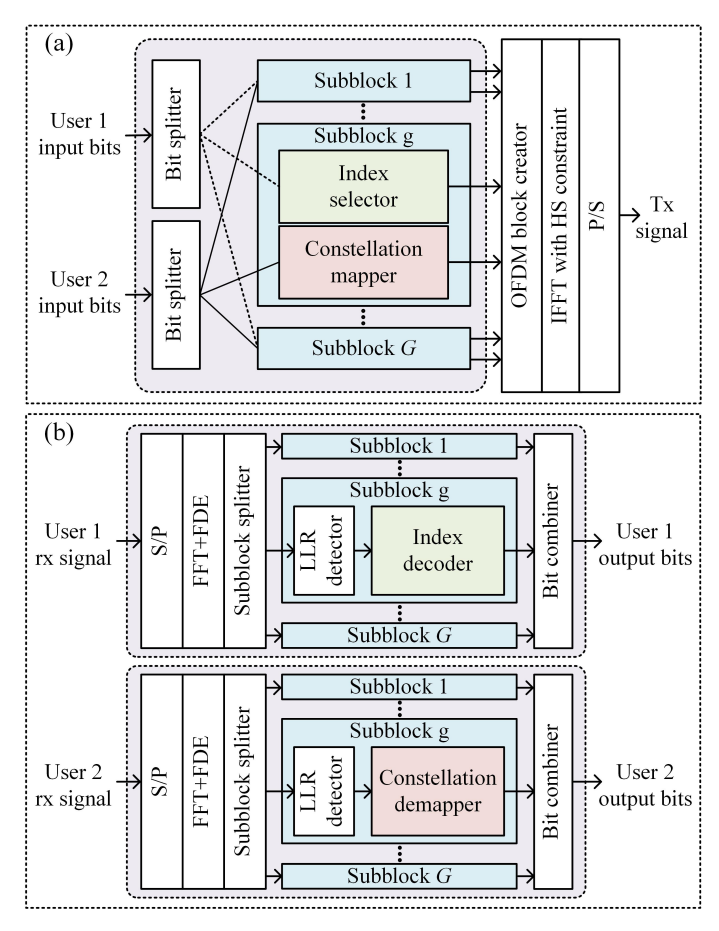


Fig. 1. Schematic diagram of the two-user VLC-IoMT system employing IMMA: (a) transmitter and (b) receiver.

At the receiver, as shown in Fig. 1(b), the received serial signals from both users are first converted to parallel form using serial-to-parallel (S/P) conversion. After performing fast Fourier transform (FFT) and frequency-domain equalization (FDE), the OFDM block for each user is divided into *G* subblocks using an OFDM block splitter. Within each subblock, a low-complexity log-likelihood ratio (LLR) detector is employed for signal detection. The index bits of user 1 and the constellation bits of user 2 are recovered directly via the index decoder and constellation demapper within each subblock, respectively. Finally, the output bits of user 1 are obtained by combining the index bits through a bit combiner, while the output bits of user 2 are generated by combining the constellation bits.

In the two-user VLC-IoMT system employing IMMA, the input data of user 1 is transmitted as index-domain bits, which is more suited for IoT devices with limited computing capacity and low data rate requirements. On the other hand, the input data of user 2, transmitted as constellation-domain bits, caters to mobile devices that require higher communication data rates. Specifically, in each sub-block of length N, typically only k subcarriers are activated to map constellation symbols, which are selected from a constellation set $M = [S_1, S_2, \ldots, S_M]$ with size M. Additionally, the indices of the N-k inactive subcarriers can be used to transmit index-domain information. Table. 1 presents the mapping rules for IMMA where N = 4 and k = 3. At the receiver, LLR detection is generally employed for the received signals due to its relatively low computational complexity. Assuming that y^n_β ($\beta = 1, \ldots, G$; $\eta = 1, \ldots, N$) represents the input signal to the LLR detector, the corresponding LLR values for the β -th subblock can be calculated as follows:

$$\kappa_{\beta}^{\eta} = \ln(k) - \ln(N - k) + \frac{\left| \left(y_{\beta}^{\eta} \right) \right|^{2}}{N_{0}} + \ln \left(\sum_{m=1}^{M} \exp \left(-\frac{1}{N_{0}} \left| y_{\beta}^{\eta} - S_{m} \right|^{2} \right) \right),$$
(1)

where N_0 is the noise power. Moreover, based on the principle of IMMA, the number of index bits for user 1 in each subblock can be given by:

$$b_1 = |\log_2(C(N, k))|,$$
 (2)

where $\lfloor \cdot \rfloor$ denotes the floor operator and $C(\cdot)$ represents the binomial coefficient. Similarly, the number of constellation bits that can be carried by the constellation set M for user 2 per subblock can be determined by:

$$b_2 = k \log_2(M). \tag{3}$$

Hence, the spectral efficiency for user 1 and user 2 in each subblock can be, respectively, calculated as follows:

$$SE_1 = \frac{\left\lfloor \log_2\left(C(N,k)\right)\right\rfloor}{N},\tag{4}$$

$$SE_2 = \frac{k \log_2(M)}{N}. (5)$$

Table 1. Mapping table of IMMA for N = 4 and k = 3

Index bits	Index set for M	Subblocks
0 0	[1, 2, 3]	$[S_i, S_j, S_l, 0]$
0 1	[1, 2, 4]	$[S_i, S_j, 0, S_l]$
1 0	[1, 3, 4]	$[S_i, 0, S_j, S_l]$
1 1	[2, 3, 4]	$[0, S_i, S_j, S_l]$

Although a simple two-user case is considered in the current work, it is feasible to support more than two users using the proposed IMMA scheme. Particularly, a hybrid IMMA-OFDMA scheme can be further designed for VLC-IoMT systems with an arbitrary number of users, which can be considered as an improved OFDMA scheme with additional index bits.

3. Results and discussions

In this section, we evaluate and compare the performance of a two-user VLC-IoMT system employing the proposed IMMA scheme, as well as conventional OFDMA and NOMA schemes, through numerical simulations and hardware experiments. In both simulations and experiments,

the length of the IFFT is set to 256, with a total of 64 subcarriers (from the 2nd to the 65th) used for data modulation. Additionally, considering the trade-off between data rate and detection complexity, the length of each subblock is set to N=4 with k=3. The constellation set size is 16 (i.e., M=16), and the overall bandwidth of the system is denoted as B. Based on Eqs. (4) and (5), the corresponding spectral efficiency of user 1 and user 2 are 0.5 bits/s/Hz and 3 bits/s/Hz, respectively. To ensure a fair comparison, the data rates for both users are kept consistent across all three schemes. Therefore, the NOMA scheme modulates user 1 with 2-ary quadrature amplitude modulation (2-QAM), utilizing half of the bandwidth (B/2), while user 2 is modulated with 8-QAM and uses the full bandwidth (B). Moreover, the optimal power allocation ratio is considered for NOMA during the following simulation and experimental evaluations. In the case of OFDMA, the overall bandwidth B is evenly divided between the two users, allowing each user to access B/2 of the bandwidth. To match the data rate of the IMMA scheme, user 1 and user 2 in OFDMA are modulated using 2-QAM and 64-QAM, respectively.

3.1. Simulation results

Figure 2 illustrates the geometric configuration of the two-user VLC-IoMT system. As shown, user 1 is positioned directly beneath the LED at a vertical distance of d meters, while the separation between user 1 and user 2 is δ meters. In the simulations, d is set to 2.15 meters, and various values of δ (0.5 m, 1 m, 1.5 m, and 2 m) are chosen to investigate the impact of channel gain differences on the performance of the schemes. Additionally, the noise in the system is assumed to follow an additive white Gaussian noise (AWGN) model.

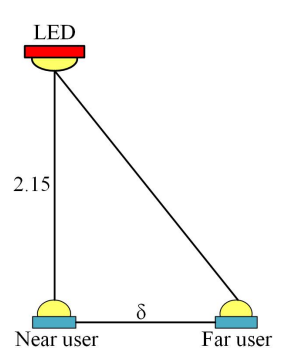


Fig. 2. The geometric configuration of the two-user VLC-IoMT system employing IMMA.

Figure 3 shows the simulated average BER of the two users versus the transmit signal-to-noise ratio (SNR) for OFDMA, NOMA, and various IMMA schemes under different user separations. In this comparison, the spectral efficiencies for user 1 and user 2 are set to 0.5 bits/s/Hz and 3 bits/s/Hz, respectively. As illustrated in Figs. 3(a)-(b), the IMMA scheme with N=4 and k=3 demonstrates the best performance, while the IMMA scheme with N=4 and k=1 shows the poorest performance among all schemes. Additionally, it can be observed that the BER performance of IMMA with N=4 and k=2 is comparable to that of OFDMA when user separations are set to 0.5 m and 1.5 m. Notably, OFDMA outperforms NOMA when the user separation is 0.5 m. However, as the user separation increases to 1.5 m, NOMA exhibits better BER performance than OFDMA due to its power allocation strategy. In the following simulation and experimental evaluations, the IMMA scheme is particularly referring to the case of IMMA with N=4 and k=3.

Figure 4 depicts the simulated BER of each user versus transmit SNR for IMMA, NOMA, and OFDMA, under different user separations. When the user separation is set to 0.5 m (i.e., $\delta = 0.5$), as shown in Fig. 4(a), both users in the IMMA scheme achieve the best BER performance,

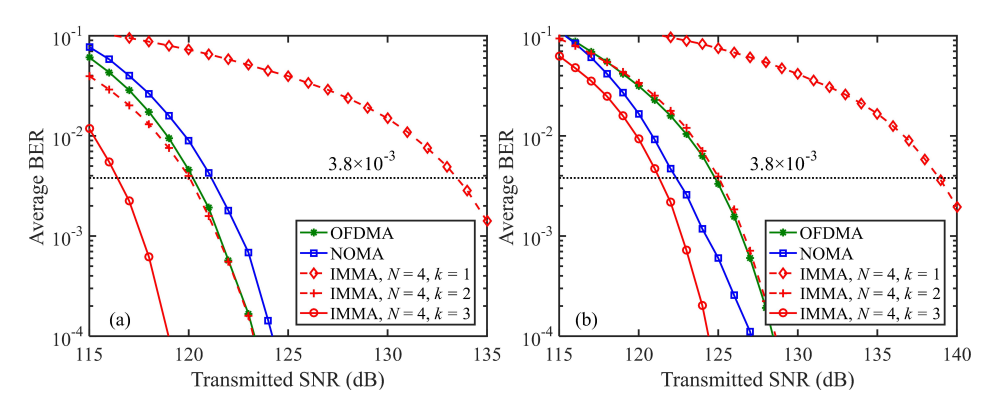


Fig. 3. Average BER vs. transmitted SNR for OFDMA, NOMA, and different IMMA schemes with (a) $\delta = 0.5$ m and (b) $\delta = 1.5$ m.

whereas the BER of the near user in the NOMA scheme is the worst due to the close proximity between users. When the user separation increases to 1.5 m, Fig. 4(b) shows a significant difference in BER performance between the two users in both the IMMA and OFDMA schemes. In contrast, the BER gap between users in the NOMA scheme is relatively smaller due to power allocation. However, the proposed IMMA scheme still outperforms NOMA, and NOMA shows better performance than OFDMA.

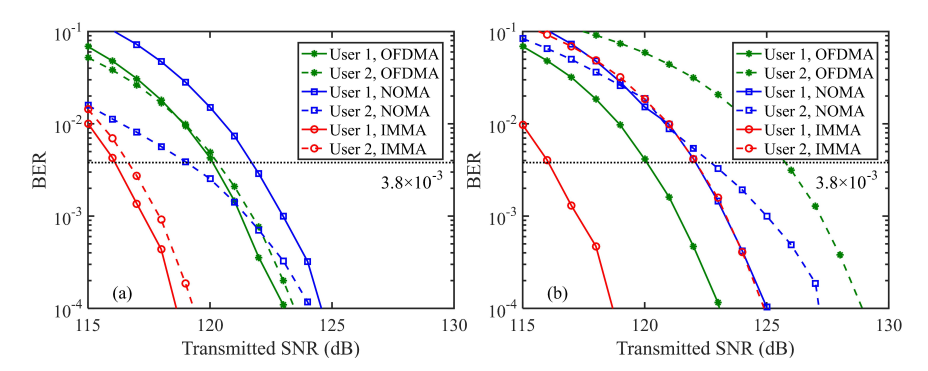


Fig. 4. BER of each user vs. transmitted SNR for OFDMA, NOMA, and IMMA with (a) δ =0.5 m and (b) δ =1.5 m.

Figure 5 presents the simulated average BER versus transmitted SNR for IMMA, NOMA, and OFDMA under different user separations. When $\delta=0.5$ m, as shown in Fig. 5(a), the required maximum SNR to achieve the 7% forward error correction (FEC) coding limit of BER = 3.8×10^{-3} for IMMA, OFDMA, and NOMA is 116.4 dB, 120.2 dB, and 121.2 dB, respectively. Therefore, IMMA outperforms OFDMA and NOMA with SNR gains of 3.8 dB and 4.8 dB, respectively. For $\delta=1$ m, as shown in Fig. 5(b), NOMA performs slightly better than OFDMA due to the significant channel gain differences between users, while IMMA still achieves the best performance, surpassing NOMA by 3.1 dB in SNR gain. As the user separation increases to 1.5 m, Fig. 5(c) shows that IMMA maintains an SNR advantage of 1 dB over NOMA. Finally, for $\delta=2$ m in Fig. 5(d), IMMA exhibits a much lower average BER compared to OFDMA, while only slightly outperforming NOMA. This is primarily because NOMA can balance the channel gain differences between users through power allocation as the distance between users increases, whereas IMMA and OFDMA are less optimized for such variations.

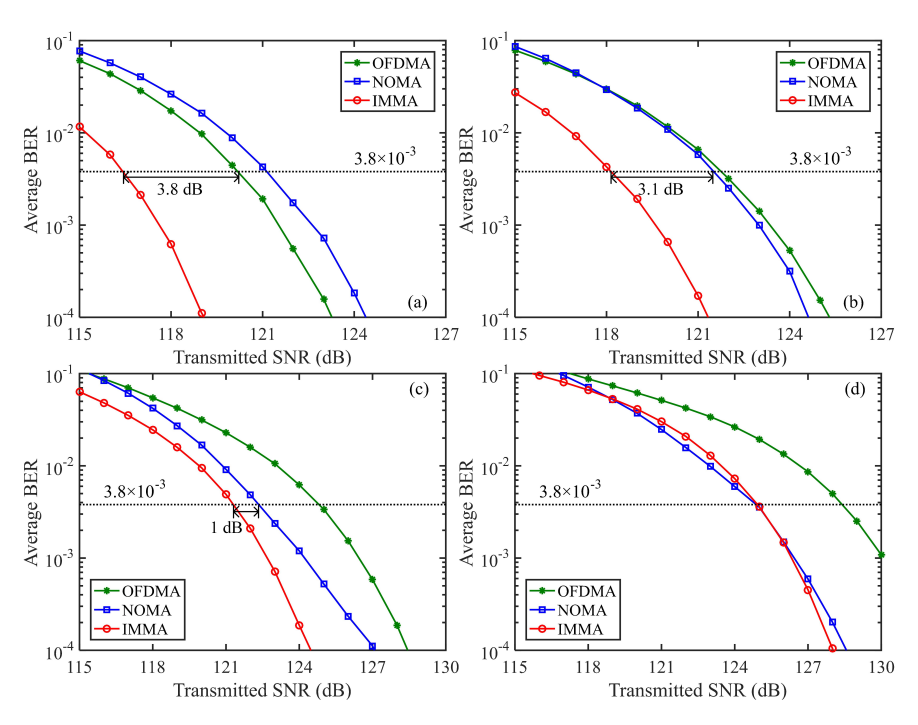


Fig. 5. Average BER vs. transmitted SNR for OFDMA, NOMA, and IMMA with (a) δ =0.5 m, (b) δ =1 m, (c) δ =1.5 m, (d) δ =2 m.

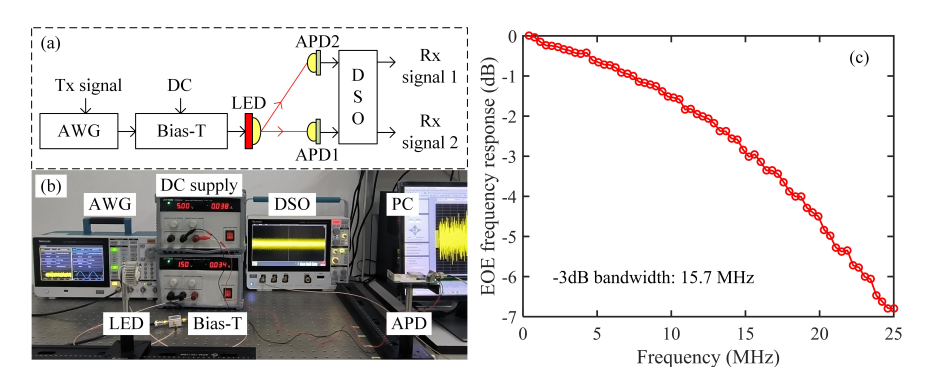


Fig. 6. (a) Experimental setup of the two-user VLC-IoMT system, (b) the photo of the overall experimental testbed and (c) EOE frequency response.

As a result, the proposed IMMA scheme not only considers the diverse QoS requirements of different users but also demonstrates superior BER performance compared to NOMA and OFDMA, making it a highly promising candidate for multi-user VLC-IoMT systems.

3.2. Experimental results

In this section, we conduct experiments to assess the performance of a practical two-user VLC-IoMT system utilizing the IMMA scheme, along with two state-of-the-art benchmark schemes, i.e., OFDMA and NOMA. The experimental setup for the two-user VLC-IoMT system is illustrated in Fig. 6(a). In this setup, the transmitted signal is initially generated offline using MATLAB and then uploaded to an arbitrary waveform generator (AWG, Tektronix AFG31102) operating at a sampling rate of 100 MSa/s. The AWG output signal has a peak-to-peak voltage

(Vpp) of 3V. Subsequently, a 34-mA DC bias current is applied to the AWG output signal through a bias tee (bias-T, MiniCircuits, ZFBT-6GW+), which is then used to drive a commercially available infrared LED with a wavelength of 850 nm, an optical power of 0.5 W and a semi-angle of 30°.

At the receiver end, each user is equipped with an avalanche photodiode (APD, Hamamatsu C12702-12) to detect the optical signal. Notably, APD 1 is positioned directly in front of the LED, while the distance between APD 2 and APD 1 varies from 5 to 20 cm. Additionally, the transmission distance between the LED and the two APDs ranges from 40 to 70 cm. The detected electrical signals are subsequently captured by a two-channel digital storage oscilloscope (DSO, Tektronix MDO32) at a sampling rate of 500 MSa/s and further processed offline using MATLAB. In the digital OFDM modulation, the IFFT length is set to 256, with 64 subcarriers (from the 2nd to the 65th) used for data modulation. Consequently, the bandwidth of the AWG output signal is approximately 25 MHz. A photo of the entire experimental setup is presented in Fig. 6(b), while Fig. 6(c) illustrates the frequency response of the system, which demonstrates a typical low-pass characteristic with a -3 dB bandwidth of around 15.7 MHz.

Figures 7(a)-(d) illustrate the measured average BER versus transmission distance for various schemes with different user separations. As observed, the BER increases progressively across all schemes as the transmission distance extends from 40 to 70 cm. Specifically, when the user separation is set to 5 cm (i.e., $\delta = 5$ cm), as shown in Fig. 7(a), the maximum transmission distances that meet the 7% FEC coding limit of BER = 3.8×10^{-3} are 47.9 cm for NOMA and 52 cm for OFDMA, while IMMA extends the maximum transmission distance to 70 cm. This results in a substantial 34.6% increase in distance compared to OFDMA. For $\delta = 10$ cm, as shown in Fig. 7(b), the maximum transmission distances achieved by OFDMA, NOMA, and IMMA

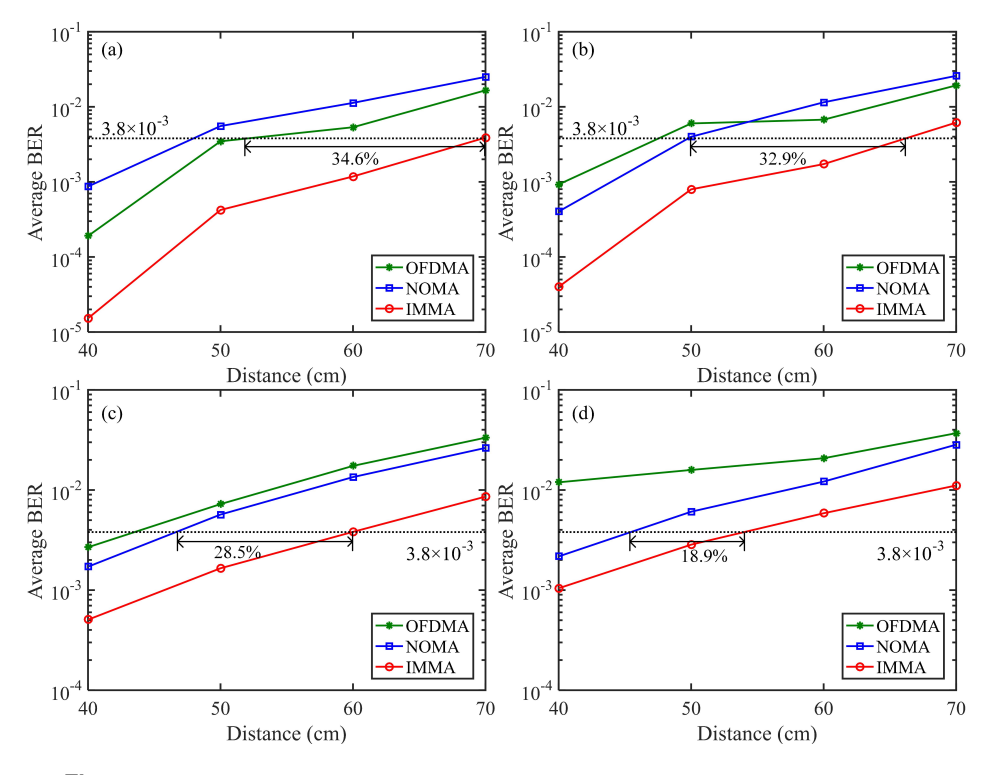


Fig. 7. Measured average BER vs. transmission distance for OFDMA, NOMA, and IMMA with (a) $\delta = 5$ cm, (b) $\delta = 10$ cm, (c) $\delta = 15$ cm, (d) $\delta = 20$ cm.

below the FEC limit are 47.5 cm, 49.8 cm, and 66.2 cm, respectively. IMMA thus outperforms NOMA by 16.4 cm, representing a 32.9% improvement in transmission distance. With the user separation increased to 15 cm, as shown in Fig. 7(c), the maximum transmission distances are 43.5 cm for OFDMA, 46.6 cm for NOMA, and 59.9 cm for IMMA. This demonstrates a 28.5% improvement in distance for IMMA compared to NOMA. Lastly, for $\delta = 20$ cm, as depicted in Fig. 7(d), OFDMA fails to meet the FEC limit within the 40–70 cm range, while NOMA reaches 45.4 cm and IMMA extends the transmission distance to 53.9 cm, achieving an 18.9% improvement over NOMA. Additionally, as user separation increases, the difference in channel gains between the users grows, leading to a progressively lower BER for NOMA compared to OFDMA, though still higher than that of IMMA. These results indicate that the proposed IMMA scheme significantly enhances the performance of practical two-user VLC-IoMT systems.

4. Conclusions

In this paper, we have proposed and investigated a novel IMMA scheme for multi-user VLC-IoMT systems. By accounting for the diverse QoS requirements among users, the IMMA scheme leverages both index symbols and constellation symbols to transmit information. Additionally, the scheme completely eliminates inter-user interference, significantly reducing the computational complexity at the receiver. Both simulations and experiments were conducted to evaluate and compare the performance of a practical two-user VLC-IoMT system using IMMA, NOMA, and OFDMA schemes, confirming that the IMMA scheme delivers substantial performance improvements. Specifically, IMMA consistently achieves the lowest BER under various user separations. Notably, when the user separation is relatively small, IMMA significantly outperforms both OFDMA and NOMA, offering up to 3.8 dB and 4 dB SNR gains in numerical simulations, as well as up to 38% and 40% increases in transmission distance in hardware experiments, respectively. Therefore, the proposed IMMA scheme presents a promising solution for practical multi-user VLC-IoMT systems. In our future work, we will further investigate the hybrid IMMA-OFDMA scheme for VLC-IoMT systems with an arbitrary number of users.

Funding. National Natural Science Foundation of China (62271091, 61901065); Natural Science Foundation of Chongqing Municipality (cstc2021jcyj-msxmX0480).

Disclosures. The authors declare no conflicts of interest.

Data availability. The data underlying the results presented in this paper are not publicly available at this time but may be obtained from the authors upon reasonable request.

References

- S. Razdan and S. Sharma, "Internet of Medical Things (IoMT): Overview, emerging technologies, and case studies," IETE Technical Review 39(4), 775–788 (2022).
- J. Sun, F. Khan, J. Li, et al., "Mutual authentication scheme for the device-to-server communication in the Internet of Medical Things," IEEE Internet Things J. 8(21), 15663–15671 (2021).
- K. Wang, T. Song, Y. Wang, et al., "Evolution of short-range optical wireless communications," J. Lightwave Technol. 41(4), 1019–1040 (2023).
- B. Han, J. Yang, K. Sun, et al., "Experimental demonstration of blue light transmitter with 30 Mbps modulated rate and 1.69 W optical power for underwater wireless optical communication based on chip-on-board light-emitting diode array," Opt. Eng. 61(05), 056106 (2022).
- Z. Zhang, Y. Xiao, Z. Ma, et al., "6G wireless networks: Vision, requirements, architecture, and key technologies," IEEE Veh. Technol. Mag. 14(3), 28–41 (2019).
- N. Chi, Y. Zhou, Y. Wei, et al., "Visible light communication in 6G: Advances, challenges, and prospects," IEEE Veh. Technol. Mag. 15(4), 93–102 (2020).
- S. Muhammad, S. H. A. Qasid, S. Rehman, et al., "Visible light communication applications in healthcare," Technology and Health Care 24(1), 135–138 (2016).
- 8. K. H. Lim, H. S. Lee, and W. Y. Chung, "Multichannel visible light communication with wavelength division for medical data transmission," Journal of Medical Imaging and Health Informatics 5(8), 1947–1951 (2015).
- 9. S. Caputo, G. Borghini, S. Jayousi, *et al.*, "Visible light communications for healthcare applications: Opportunities and challenges," in *IEEE International Symposium on Medical Information and Communication Technology (ISMICT)*, (2023), pp. 1–6.

- H. Jin, "Nanosensor-based flexible electronic assisted with light fidelity communicating technology for volatolomics-based telemedicine," ACS Nano 14(11), 15517–15532 (2020).
- Z. Zeng, M. Dehghani Soltani, Y. Wang, et al., "Realistic indoor hybrid WiFi and OFDMA-based LiFi networks," IEEE Trans. Commun. 68(5), 2978–2991 (2020).
- C. Chen, Y. Tang, Y. Cai, et al., "Fairness-aware hybrid NOMA/OFDMA for bandlimited multi-user VLC systems," Opt. Express 29(25), 42265–42275 (2021).
- 13. M. A. Arfaoui, A. Ghrayeb, C. Assi, *et al.*, "CoMP-assisted NOMA and cooperative NOMA in indoor VLC cellular systems," IEEE Trans. Commun. **70**(9), 6020–6034 (2022).
- 14. Y. R. Tang, C. Chen, C. W. He, *et al.*, "Joint in-phase and quadrature non-orthogonal multiple access for multi-user VLC," J. Lightwave Technol. **42**(20), 7219–7228 (2024).
- C. Chen, S. Fu, X. Jian, et al., "NOMA for energy-efficient LiFi-enabled bidirectional IoT communication," IEEE Trans. Commun. 69(3), 1693–1706 (2021).
- A. A. Purwita, A. Yesilkaya, M. Safari, et al., "Generalized time slot index modulation for optical wireless communications," IEEE Trans. Commun. 68(6), 3706–3719 (2020).
- F. Ahmed, Y. Nie, C. Chen, et al., "DFT-spread OFDM with quadrature index modulation for practical VLC systems," Opt. Express 29(21), 33027–33036 (2021).
- X. Zhang, Z. Zeng, P. Du, et al., "Intelligent index recognition for OFDM with index modulation in underwater OWC systems," IEEE Photonics Technol. Lett. 36(20), 1249–1252 (2024).
- E. Basar, U. Aygolu, E. Panayirci, et al., "Orthogonal frequency division multiplexing with index modulation," IEEE Trans. Signal Process. 61(22), 5536–5549 (2013).
- E. Başar and E. Panayırcı, "Optical OFDM with index modulation for visible light communications," in IEEE International Workshop on Optical Wireless Communications (IWOW), (2015), pp. 11–15.
- C. Chen, X. Deng, Y. Yang, et al., "Experimental demonstration of optical OFDM with subcarrier index modulation for IM/DD VLC," in Asia Communications and Photonics Conference (ACP), (2019), pp. 1–3.
- 22. Y. Zhao, C. Chen, X. Zhong, *et al.*, "Enhancing OFDM with index modulation using heuristic geometric constellation shaping and generalized interleaving for underwater VLC," Opt. Express **32**(8), 13720–13732 (2024).